J. Fluid Mech. (1979), *vol.* 92, *part* 2, *pp.* 241–267
Printed in Great Britain

Gravity–capillary waves with edge constraints

By T. BROOKE BENJAMIN† AND JOHN C. SCOTT
Fluid Mechanics Research Institute, University of Essex, Colchester CO4 3SQ

(Received 3 August 1978)

This paper presents a theoretical and experimental investigation into a novel class of water-wave motions in narrow open channels. The distinctive condition on these motions is that the lines of contact between the free surface and the sides of the channel are fixed, which condition bears crucially on the hydrodynamic effects of surface tension. Most of the account concerns travelling waves in channels of rectangular cross-section that are exactly brimful, but the relevance of this prototype to other, more usual situations is explained with reference to the phenomenon of contact-angle hysteresis.

In § 2 a linearized theory is developed which poses an eigenvalue problem of unusual kind. Unlike the familiar and much simpler problem corresponding to mobile lines of contact at which the free surface remains horizontal, the new problem has no explicit solution and the edge conditions are not automatically compatible with the kinematic conditions at the solid boundaries. Treatment by functional analytic methods is necessary to verify that solutions exist having physically appropriate properties, but this approach gives a final bonus in securing comparatively easy estimates for some of these properties. A variational characterization of the eigenvalues is used to settle questions of existence and the ordering of possible wave modes, and finally to establish approximate formulae relating wavelength to frequency.

In § 3 experiments are reported which were performed with clean water filling three channels made of Perspex. Over continuous ranges of frequency, delimited so that only the fundamental progressive-wave mode was generated, wavelengths were measured by an electronic technique. The measurements agree well with the theoretical predictions, diverging markedly from behaviour to be expected in the absence of edge constraints.

Appendix A outlines a supplementary theoretical argument proving that the first eigenvalue of the problem treated in § 2 is always simple. Appendix B reviews three generalizations of the theory.

1. Introduction

The class of wave motions that is the subject of this paper has apparently received little attention so far. A heavy liquid with uniform surface tension is contained in a horizontal open channel, and the novel feature to be investigated is that the lines of contact between the free surface and the sides of the channel are fixed. Waves are transmitted along the channel, disturbing the liquid from a state of rest, and the relationship between their frequency and wavelength depends on the edge constraints.

† Present address: Mathematical Institute, Oxford OX1 3LB.

0022-1120/79/4231-6470 $02.00 © 1979 Cambridge University Press

It may at once be appreciated that the stiffening effect of surface tension is magnified by these constraints, so that speeds of propagation are generally larger than they would be if the free surface were able to move up and down the sides of the channel.

A linearized theory of progressive waves in the new class is presented in § 2. It is developed for the particular case of a brimful channel with rectangular cross-section, and the use of a variational principle leads to explicit estimates of wave properties in this case. The theory is considerably harder than the standard theory for waves free from edge constraints, and explicit solutions are unobtainable. Generalizations of the theory applying to channels of arbitrary cross-section, to cases where the undisturbed free surface is not flat and to standing waves in closed basins are summarized in an appendix. Other theoretical aspects, in particular concerning the nonlinear problem for progressive waves, will be reported elsewhere.

Experimental measurements are reported in § 3 which agree well with the predictions of the theory. The experiments were designed to ensure fixed contact lines, and so they are not immediately comparable with other, more familiar situations where gravity–capillary waves are observable. A wider bearing of the present investigation may be indicated, however, by the following notes about observations that were preliminary to those detailed in § 3.

The investigation was in fact suggested by consideration of certain discrepancies encountered in the measurement of wave propagation on clean water in a Perspex channel of width 100 mm, five to twenty times the widths of the channels used for the present experiments. At the vertical sides of the channel, the water surface had menisci of height about 2 mm, leaving ample freeboard above. Measured values of phase speed at various frequencies were found consistently to be somewhat greater than those calculated according to the standard linearized theory of long-crested waves (as will be recalled in § 3.2 for purposes of comparison); and careful measurements of surface tension, together with measurements of wave attenuation, indicated that this effect was unlikely to have been caused by surface contamination.

A more likely reason appeared to be associated with the contact zones at the sides of the channel. In general, for surface-clean water placed in a Perspex vessel that has been thoroughly cleaned and is free of scratches, the line of contact between the free surface of the water and the Perspex may be observed to remain stationary when the surface is gently agitated. There are thus temporal variations in the contact angle, being consistent with the hysteresis of contact angle that is found to occur between water and Perspex, as in fact occurs to a measurable extent between most liquids and all but a few painstakingly prepared solid surfaces (for typical values, see Stepanov, Volyak & Tarlakov 1977). The term hysteresis is otherwise used to refer to the difference in the observed contact angle accordingly as the water is advancing or receding across the solid surface, but here the term refers rather to the difference in the limiting angles that the water surface makes with a static contact line under forces tending to move it respectively forward or backward. We note that, if there were no such hysteresis, raindrops would not stick to a windowpane.

It may accordingly be expected that, provided the wave amplitude is small enough for the contact angle to remain between these limiting values, water waves will not displace the contact line on a Perspex wall. In a wide channel with Perspex walls such as that mentioned above, the effects of fixed contact lines are largely confined to regions near the walls, there distorting the planform of progressive waves that appear more or less long-crested in the central part of the span. Although wave speeds may be appreciably affected, as we noted above, the effects in question are then hardly more than residual complications of a two-dimensional (i.e. spanwise uniform) wave system. In a sufficiently narrow channel, in the other hand, these effects become predominant, and wave speeds are unmistakably larger than those of corresponding two-dimensional waves.

The experiments reported in § 3 were made with three Perspex channels of widths roughly 4, 10 and 20 mm. To simulate the theoretical model studied in § 2, each channel was filled precisely to the level of the horizontal top surfaces of the Perspex walls. The contact lines were thus located along the sharp edges of right-angled corners, where, as the net outcome of microscopic processes, the angle spanned by contact hysteresis was effectively increased by 90° above the value for a plane solid surface. It was found that quite large waves could be generated in the water without dislodgement of the contact lines, which certainly remained fixed under the action of the small-amplitude waves measured in the main experiments.

The problem here investigated may be likened to various other 'hydroelastic' problems where a surface with known bending stiffness is subject to hydrodynamic loading. We are aware of few previous studies that are directly relevant, although Walbridge & Woodward (1970) reported some experimental observations on progressive waves in narrow brimful channels. They found that 'the meniscus was irregular at the edges', a complication avoided in our experiments by the use of carefully cleaned water and Perspex, and their measurements of wavelength as a function of channel width for a fixed frequency encountered large variations on repetition from day to day. An empirical formula roughly correlating the experimental results was proposed by them, but it is in obvious respects inconsistent with the hydrodynamical problem. The present theoretical predictions also fall within the range of their experimental results. We have seen some theoretical work comparable with ours in an unpublished M.Sc. thesis by R. J. Astley (1969), who correctly formulated the linearized problem for two-dimensional standing waves in a liquid filling a deep rectangular trough and having a free surface with fixed edges. His method of approximate solution appears inexpedient, however, in that it entails a somewhat elaborate and slowly convergent iteration. The present treatment proceeds on quite different lines.

2. Theory

The theoretical model is illustrated in figure 1. A liquid completely fills a straight horizontal open channel of rectangular cross-section with uniform breadth b and depth h. When at rest, the free surface of the liquid is everywhere horizontal, making contact with the side-walls at sharp edges. Cartesian axes (x, y, z) are taken with origin in the free surface at one side-wall, with y upwards and z along the channel which is unbounded lengthwise. The liquid is assumed to be inviscid and incompressible, and to have a constant surface tension denoted by $\rho\gamma$, where ρ is the density. The propagation of free waves along the channel is to be investigated, subject to the condition that contact between the free surface and side-walls is fixed in the horizontal lines

$$(x, y) = (0, 0) \quad \text{and} \quad (x, y) = (b, 0).$$

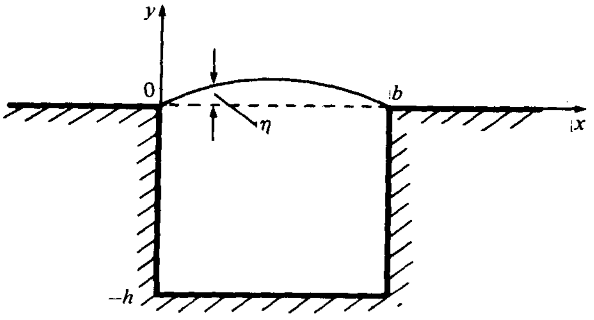

FIGURE 1. Cross-section of channel.

2.1. *Equations of motion*

Considering the possibility of a sinusoidal travelling wave, we suppose the equation of the perturbed free surface to have the form

$$y = \eta(x,z,t) = \epsilon f(x)\, e^{i(\omega t - \alpha z)} \tag{1}$$

with

$$f(0) = 0 \quad \text{and} \quad f(b) = 0. \tag{2}$$

Here the amplitude ϵ, frequency ω and wavenumber α are constants, and $|\epsilon|$ is assumed to be small enough to justify linearized approximations to the boundary conditions applying at the free surface. Having supposedly been started from rest by conservative forces, the motion in the liquid is therefore irrotational, and an appropriate form for its velocity potential is

$$\phi = i\omega\epsilon\Phi(x,y)\, e^{i(\omega t - \alpha z)}.$$

Since the liquid is incompressible, ϕ is a harmonic function of (x, y, z). Hence the function $\Phi(x,y)$ satisfies

$$\Phi_{xx} + \Phi_{yy} - \alpha^2\Phi = 0 \tag{3}$$

in the cross-sectional domain Ω, whose closure $\bar{\Omega}$ can be taken to be $[0,b] \times [-h, 0]$ for the linearized theory.

The boundary conditions on Φ are as follows. For the normal component of velocity to vanish everywhere on the bottom and side-walls, it is required that

$$\Phi_y(x, -h) = 0 \quad \forall\, x \in [0,b], \tag{4}$$

$$\Phi_x(0,y) = 0, \quad \Phi_x(b,y) = 0 \quad \forall\, y \in [-h, 0]. \tag{5}$$

The linearized kinematical condition at the free surface is

$$\eta_t = \phi_y(x, 0, z, t),$$

which requires that

$$\Phi_y(x,0) = f(x) \quad \forall\, x \in [0,b]. \tag{6}$$

The linearized approximation to the total curvature of the free surface is $\eta_{xx} + \eta_{zz}$, so that the pressure in the liquid just beneath the surface is approximately $-\rho\gamma(\eta_{xx} + \eta_{zz})$. Hence the linearized dynamical condition is

$$g\eta - \gamma(\eta_{xx} + \eta_{zz}) + \phi_t(x, 0, z, t) = 0$$

(cf. Lamb 1932, §227), requiring that

$$(g + \gamma\alpha^2) f(x) - \gamma f''(x) = \omega^2\Phi(x, 0) \quad \forall\, x \in [0,b]. \tag{7a}$$

We define an operator B such that a function f given on $[0, b]$ is transformed into $Bf = \Phi(x, 0)$, where $\Phi(x, y)$ is the unique solution of the Neumann problem comprised by (3) and the boundary conditions (4), (5) and (6). Thus (7 a) can be rewritten

$$(g+\gamma\alpha^2)f(x)-\gamma f''(x) = \omega^2 Bf(x). \tag{7b}$$

This completes the specifications of the dynamical problem, and we proceed to investigate the possible values of ω corresponding to given real values of α.

2.2. *Simplified problem*

When the edge conditions (2) are relaxed, the problem has simple solutions which are well known. These are now recalled in order to introduce several facts that will be needed in the treatment of the original problem. Using tildes to connote the simplified problem and writing $\beta = \pi/b$, we observe that if the function $f(x)$ in (1) is one of

$$\tilde{f}_m = \cos(m\beta x) \quad (m = 0, 1, 2, \ldots), \tag{8}$$

then the unique solution of (3) satisfying (4), (5) and (6) is

$$\tilde{\Phi}_m = \frac{\cos(m\beta x)\cosh k_m(y+h)}{k_m \sinh k_m h}, \tag{9}$$

where $k_m = (\alpha^2+m^2\beta^2)^{\frac{1}{2}}$. Hence, to satisfy the remaining boundary condition (7 a), $\tilde{\omega}^2$ must have the value

$$\tilde{\omega}_m^2 = (k_m g + k_m^3 \gamma)\tanh k_m h. \tag{10}$$

In each of the possible wave modes corresponding to $m = 0, 1, 2, \ldots$, the moving free surface remains normal to the side-walls, and $m = 0$ recovers the case of a two-dimensional wave motion [cf. Lamb 1932, p. 463, equation (4)]. For each real value of α, the frequencies $\tilde{\omega}_m(\alpha)$ according to (10) satisfy $0 \leqslant \tilde{\omega}_0^2(\alpha) < \tilde{\omega}_1^2(\alpha) < \tilde{\omega}_2^2(\alpha) < \ldots$, and their positive values are monotonic increasing with $|\alpha|$. The positive phase velocity

$$\tilde{c}_0 = \tilde{\omega}_0/\alpha$$

and group velocity $d\tilde{\omega}_0/d\alpha = \tilde{c}_0+\alpha\, d\tilde{c}_0/d\alpha$ have the limit $(gh)^{\frac{1}{2}}$ as $\alpha \to 0$, and are asymptotic to $(\alpha\gamma)^{\frac{1}{2}}$ and $\frac{3}{2}(\alpha\gamma)^{\frac{1}{2}}$ as $\alpha \to \infty$. If $h < (3\gamma/g)^{\frac{1}{2}}$, which value is about 4·7 mm for clean water, $\tilde{c}_0(\alpha)$ is monotonic increasing with $|\alpha|$. If $h > (3\gamma/g)^{\frac{1}{2}}$, $\tilde{c}_0(\alpha)$ has a minimum at a non-zero value of $|\alpha|$, and accordingly the group velocity is less than $\tilde{c}_0$ for positive $|\alpha|$ less than the optimum. For every $m \geqslant 1$, $\tilde{\omega}_m^2(\alpha)$ has a positive limit as $\alpha \to 0$, applying to the standing waves independent of z that are possible in these modes. Each of the phase velocities $\tilde{c}_m(\alpha)$ has a minimum at a respective non-zero value of $|\alpha|$.

2.3. *Properties of the operator B*

For use later, it will be helpful to note the following facts about the Neumann problem comprised by (3)–(6). When the function $f(x)$ in (6) has the form (8), the problem is immediately soluble, determining the function $\Phi(x, 0) = Bf$. Thus, according to the solution (9), we have that $Bf_m = \mu_m f_m$, where

$$\mu_m = k_m^{-1}\coth k_m h. \tag{11}$$

The operator B is linear, and consequently, for an arbitrary function expressible by a half-range cosine series on $[0, b]$ that is, for

$$u(x) = \sum_{m=0}^{\infty} A_m \cos m\beta x, \tag{12}$$

we have that
$$Bu(x) = \sum_{m=0}^{\infty} \mu_m A_m \cos m\beta x. \tag{13}$$

It is now required to define suitable domains and co-domains for B.

For the real space $L^2(0, b)$, denote the inner product by

$$(u, v)_0 = \frac{1}{b}\int_0^t uv\,dx.$$

With respect to any given non-negative integer s, we consider the space of real, *even*, periodic functions with period $2b$ that belong to $L^2(0, b)$ and have derivatives $D^l u$ also in L^2 for $l \leqslant s$. With the inner product

$$(u, v)_s = \sum_{l=0}^{s} \binom{s}{l} \beta^{-2l}(D^l u, D^l v)_0, \tag{14}$$

this is a Hilbert space, and according to Parseval's equality an alternative expression for the norm $\|u\|_s = [(u, u)_s]^{\frac{1}{2}}$ is

$$\|u\|_s = \left\{\sum_{m=0}^{\infty} (2\epsilon_m)^{-1}(1+m^2)^s A_m^2\right\}^{\frac{1}{2}}, \tag{15}$$

where $\epsilon_0 = \frac{1}{2}$, $\epsilon_m = 1$ for $m \geqslant 1$, and the $A_m = 2\epsilon_m(u, \cos m\beta x)_0$ are the coefficients of the Fourier cosine series that represents u. Related to this space and particularly needed for what follows, $\bar{H}^s$ is defined to be the space of (equivalence classes of) functions on $[0, b]$ representable as half-range cosine series such that the infinite sum in (15) converges. With the norm (15) and corresponding inner product, $\bar{H}^s$ is also a Hilbert space; and if its elements, defined on $[0, b]$, are arbitrarily extended to the whole of $\mathbb{R}$ as even periodic functions, in this guise they recover those of the first space and admit the alternative inner product (14). By means of (15), the definition of $\bar{H}^s$ can evidently be extended to cases where the real number s is other than a non-negative integer, and this generalization will be needed particularly in appendix B. An important fact to be used in what follows is that $\bar{H}^s \subset C^N[0, b]$ if $s > N + \frac{1}{2}$ $(N = 0, 1, 2, \ldots)$. In other words, the attribution $u \in \bar{H}^s$ with $s > N + \frac{1}{2}$ implies that the equivalence class of u contains a function whose Nth derivative is a continuous function on $[0, b]$ (Adams 1975, p. 97).

The positive numbers μ_m $(m = 0, 1, 2, \ldots)$, which are the (simple) eigenvalues of B, are monotonic decreasing with m and $\mu_m \sim m^{-1}$ as $m \to \infty$. Hence (14) shows that if $u \in \bar{H}^s$, then $Bu \in \bar{H}^{s'}$ for $s' \leqslant s + 1$. In fact the range of B from $\bar{H}^s$ is $\bar{H}^{s+1}$, and B is injective since no eigenvalue is zero. Thus $B : \bar{H}^s \to \bar{H}^{s+1}$ is a bijection.

It is also noteworthy that B is self-adjoint $\bar{H}^s \to \bar{H}^s$, a fact made plain by Parseval's equality referred to the explicit representation (13) of B. Applied to the Neumann problem whereby B was originally defined, Green's theorem shows that

$$(f, Bf)_0 = \frac{1}{b}\int_\Omega (\Phi_x^2 + \Phi_y^2 + \alpha^2\Phi^2)\,dx\,dy, \tag{16}$$

and we may now appreciate that this integral exists whenever $f \in \bar{H}^s$ with $s \geqslant -\frac{1}{2}$ (cf. below and appendix B).

Finally, we note that B is a positive operator in the sense that, if $u \geqslant 0$ on $[0, b]$, then Bu has the same property. This fact may be demonstrated by the maximum principle that applies to the elliptic differential equation (3), showing that a negative infimum of the boundary values of Φ is incompatible with non-negative values of the (outward) normal derivative (cf. Protter & Weinberger 1967, chap. 2, § 3). In the present context, however, the following demonstration is more instructive.

In the sense of distributions, the solution $\Phi(x, y)$ of the Neumann problem (3)–(6) can be immediately inferred to exist as an element of the Sobolev space $H^1(\Omega)$, having a trace on ∂D that belongs to $H^{\frac{1}{2}}(\partial\Omega)$ (see Lions & Magenes 1968, chap. 1, §8). The solution is specified by

$$\mathscr{F}(\Phi, f) = \min_{\xi \in H^1(\Omega)} \mathscr{F}(\xi, f), \tag{17}$$

where

$$\mathscr{F}(\xi, f) = \int_\Omega \tfrac{1}{2}(\xi_x^2 + \xi_y^2 + \alpha^2 \xi^2)\, dx\, dy - \int_0^b \xi(x, 0) f\, dx$$

is defined as a coercive, lower semi-continuous functional on $H^1(\Omega)$, therefore achieving the minimum (17), provided that $f \in H^{-\frac{1}{2}}(0, b)$ (cf. Lions & Magenes, chap. 2, § 9). Since the solution thus satisfies

$$\int_\Omega (\xi_x \Phi_x + \xi_y \Phi_y + \alpha^2 \xi \Phi)\, dx\, dy - \int_0^t \xi(x, 0) f\, dx = 0$$

for every $\xi \in H^1(\Omega)$, it is evidently unique, and with $\xi = \Phi$ this equality shows that

$$\mathscr{F}(\Phi, f) = -\frac{1}{2}\int_0^t \Phi(x, 0) f\, dx = -\tfrac{1}{2} b (f, Bf)_0, \tag{18}$$

which according to (16) is negative unless f is null. Hence, if f is (a.e.) non-negative and not null, then $\Phi(x, 0) = Bf$ must have positive values on some part of the support of f whose measure is positive. Supposing that Φ is not non-negative a.e. in $\Omega \cup \partial\Omega$, we have $|\Phi|$ distinct from Φ and also an element of $H^1(\Omega)$ (cf. Stampacchia 1963). Moreover, the component of $\mathscr{F}$ quadratic in Φ is the same for $|\Phi|$. We therefore have

$$\mathscr{F}(|\Phi|, f) \leqslant \mathscr{F}(\Phi, f),$$

which contradicts the previous conclusion that Φ is the unique minimizer of $\mathscr{F}$. Thus it is proved that $Bf \geqslant 0$ if $f \geqslant 0$.

An obvious extension of the argument shows that if $f \geqslant 0$ (a.e.), then Bf is positive where f is positive. It may be shown otherwise that Bf is in fact positive throughout $[0, b]$ if f is not null and $f \geqslant 0$ (see appendix A), but this result will not be needed at present.

2.4. *Eigenvalue problem including edge conditions*

When the conditions (2) are imposed, the problem represented by equation (7b) becomes more complicated, and care is needed to verify that eigensolutions f exist. We shall take advantage of what was shown above about B as an operator in the spaces $\bar{H}^s$, but we shall also need to consider spaces $\hat{H}^s$ whose elements defined on $[0, b]$ are representable as half-range sine series with corresponding rates of convergence.

Let $\hat{H}^1$ denote the linear manifold in $\bar{H}^1$ consisting of those elements whose equivalent continuous functions $u(x)$ satisfy $u(0) = u(b) = 0$. The respective sequences of cosine coefficients $\{A_m\}$, which plainly belong to l^1 in view of (15) with $s = 1$, accordingly satisfy

$$\mathscr{L}_1(u) = \sum_{m=0}^{\infty} A_m = 0,$$

and

$$\mathscr{L}_2(u) = \sum_{m=0}^{\infty} (-1)^m A_m = 0.$$

Since $\mathscr{L}_1$ and $\mathscr{L}_2$ are defined as linear functionals over $\hat{H}^1$, it follows that $\hat{H}^1$ is a subspace of $\bar{H}^1$ and consequently contains a countable orthogonal basis of its own. Such a basis is evidently $\{\sin n\beta x\}$ $(n = 1, 2, 3, \ldots)$. Besides (15), a third alternative expression for the norm in $\hat{H}^1$ is therefore

$$\|u\|_1 = \left\{\sum_{n=1}^{\infty} (1+n^2)\, a_n^2\right\}^{\frac{1}{2}}, \tag{19}$$

where $a_n = 2(u, \sin n\beta x)_0$, and the elements of $\hat{H}^1$ are the same on $[0, b]$ as those of the space of *odd* periodic functions having inner product (14) with $s = 1$. Spaces $\hat{H}^s$ with other values of the index s can similarly be defined. Note that $\hat{H}^1$ is a proper subspace of $\bar{H}^1$, but $\hat{H}^0$ is identical with $\bar{H}^0$. Note also that $\bar{H}^s \subset \hat{H}^0$ for $s = 1, 2, \ldots$, but the $\bar{H}^s$ are not included in any narrower space $\hat{H}^s$ with integer s. This fact is shown by the example of the function $u = 1$ common to all the spaces $\bar{H}^s$, although it belongs to $\hat{H}^s$ only if $s < \frac{1}{2}$.

Now, a weak solution of (7*b*) is defined to be an element $f \in \hat{H}^1$ such that

$$\int_0^b \{(g+\gamma\alpha^2)\, uf + \gamma u'f'\}\, dx = \omega^2 \int_0^b uBf\, dx \tag{20a}$$

is satisfied for every $u \in \hat{H}^1$. This equality can be rewritten in the form

$$\lambda\{P(u,f)_1 + Q(u,f)_0\} = (u, Bf) \quad \forall\, u \in \hat{H}^1 \tag{20b}$$

with

$$\lambda = 1/\omega^2,$$

$$P = \max\{\gamma\beta^2, (g+\gamma\alpha^2)\} > 0,$$

$$Q = |\gamma\beta^2 - (g+\gamma\alpha^2)| \geqslant 0;$$

and it is evidently satisfied if f is a solution of (7*b*) that is twice continuously differentiable on $]0, b[$ and satisfies (2). The existence of weak solutions corresponding to eigenvalues $\lambda_1 > \lambda_2 \geqslant \lambda_3 \geqslant \ldots > 0$ (each, after λ_1, repeated a number of times equal to its multiplicity) will first be verified, and then they will be shown to have sufficient regularity to satisfy (7*b*) pointwise.

First, the fact that the eigenvalues must all be real and positive follows immediately from (20*b*). Supposing $1/\omega^2$ to be complex, generalizing $\hat{H}^1$ to be a complex space and then taking u in (20*b*) to be the complex conjugate of f, one arrives at a contradiction. With $u = f$ (real) in (20*b*), positivity of the eigenvalues is shown by (16).

Existence of the first eigensolution. It will appear that a characterization of the first eigenvalue is

$$\lambda_1 = \max_{u \in \Lambda_1} F(u), \tag{21}$$

where $F(u) = (u, Bu)_0$ and Λ_1 is the subset of $\hat{H}^1$ comprised by those elements satisfying

$$G(u) = P\|u\|_1^2 + Q\|u\|_0^2 = 1. \tag{22}$$

Since $\hat{H}^1 \subset \bar{H}^1$, we know from the discussion in § 2.3 that $B(\hat{H}^1) \subset \bar{H}^2 \subset C^1[0, b]$, which confirms that the quadratic functional F is defined over $\hat{H}^1$. Furthermore, although B is clearly not a self-adjoint operator from $\hat{H}^1$ into itself (i.e., if $u \in \hat{H}^1$, the continuous function equivalent to Bu is generally not zero at $x = 0, b$), we nevertheless have that

$$(u, Bv)_0 = (v, Bu)_0 \quad \forall\, u, v \in \hat{H}^1. \tag{23}$$

It follows that the equality (20*b*) is necessary for any $f \in \Lambda_1$ to realize a stationary value of F subject to (22). The existence of a weak solution $f_1 \in \Lambda_1$ is therefore assured by showing that the maximum (21) is achieved.

The argument proceeds on standard lines. Exemplifying a property shared by every symmetric bilinear functional over a Hilbert space, the one in (23) has the representation

$$(u, Bv)_0 = (u, \mathscr{B}v)_1 \quad \forall\, u, v \in \hat{H}^1,$$

where $\mathscr{B}$ is a self-adjoint operator $\hat{H}^1 \to \hat{H}^1$ which is the gradient of $\frac{1}{2}F$ in $\hat{H}^1$. Although we yet have no explicit representation of B as an operation on sine series, there is another, crucial property of $\mathscr{B}$ that can at once be guaranteed in abstract. This operator is evidently expressible in the form

$$\mathscr{B} = A \circ B,$$

where

$$A \equiv (I - \beta^{-2}D^2)^{-1}$$

is just the symmetric operator determined in the spaces $\hat{H}^s$ by $(u, v)_s = (u, Av)_{s+1}$: thus, if

$$v = \sum_{n=1}^{\infty} a_n \sin n\beta x, \tag{24}$$

then

$$Av = \sum_{n=1}^{\infty} (1 + n^2)^{-1} a_n \sin n\beta x.$$

Plainly, A is a bijection $\hat{H}^s \to \hat{H}^{s+2}$ for arbitrary s. On the other hand, we already know that $B(\hat{H}^1) \subset \bar{H}^2$, and $\bar{H}^2 \subset \hat{H}^0$. Hence we conclude that $\mathscr{B}(\hat{H}^1) \subset \hat{H}^2$, which space is compactly embedded in $\hat{H}^1$. This means that $\mathscr{B}$ is a completely continuous operator $\hat{H}^1 \to \hat{H}^1$, and consequently the functional F is continuous with respect to weak convergence in $\hat{H}^1$. In other words, if $\{u_N\}$ is a sequence in $\hat{H}^1$ converging weakly to some element $f \in \hat{H}^1$ (recall that in a Hilbert space, every bounded sequence contains a subsequence with this property), then

$$\lim_{N \to \infty} F(u_N) = F(f).$$

Let $\{u_N\}$ be specifically a sequence from Λ_1 taking F to its supremum over Λ_1 as $N \to \infty$. The functional $G(u)$ introduced in (22), whose gradient in $\hat{H}_1$ is $2(PI + QA)$ with $P > 0$ and $Q \geqslant 0$, is an equivalent norm for $\hat{H}^1$, being thus strongly coercive. The sequence in question is consequently bounded, so that it or a subsequence has a weak limit f_1. The weak continuity of F therefore implies that

$$\sup_{u \in \Lambda_1} F(u) = F(f_1), \tag{25}$$

and, since F can have positive values [cf. (16)], f_1 is evidently not zero. On the other hand, the functional $G(u)$ is, like the norm, lower semi-continuous with respect to weak convergence in $\hat{H}_1$, so that

$$G(f_1) = P\|f_1\|_1^2 + Q\|f_1\|_0^2 \leqslant 1. \tag{26}$$

If inequality were the case in (26), a number $c > 1$ could be chosen to make $cf_1 \in \Lambda_1$, but then the fact that $F(cf) = c^2F(f_1) > F(f_1)$ would contradict (25). We conclude therefore that $f_1 \in \Lambda_1$ and the maximum (21) is realized by f_1. Thus the proof that the problem has a weak solution corresponding to the eigenvalue λ_1 is complete.

The positivity of the operator B as explained at the end of § 2.3 indicates that the continuous function equivalent to f_1 is non-negative; for if it were not, we would have $|f_1| \in \Lambda_1$ yet $F(|f_1|) \geqslant F(f_1)$ (cf. Stampacchia 1963). It will be shown in appendix A that $f_1 > 0$ on $]0, b[$, and that the eigenvalue $\lambda_1 = 1/\omega_1^2$ is simple.

Existence of further eigensolutions. The second eigenvalue may be characterized as

$$\lambda_2 = \max_{u \in \Lambda_2} F(u),$$

where Λ_2 is the intersection of Λ_1 with the subspace of $\hat{H}^1$ defined by

$$P(u, f_1)_1 + Q(u, f_1)_0 = 0.$$

Existence can be proved by repeating the previous argument with regard to this subspace. In general, the kth eigenvalue is given as the maximum of F achieved on Λ_k, which is the intersection of Λ_1 and the subspace defined by

$$P(u, f_i)_1 + Q(u, f_i)_0 = 0, \quad i = 1, 2, \ldots, (k-1),$$

where f_i is the eigensolution corresponding to the ith eigenvalue. Alternatively, the eigenvalues less than the first may be characterized by the minimax principle (Dunford & Schwartz 1963, p. 908).

Regularity. We have shown that $Bf_1 \in \bar{H}^2$, which implies it to be equivalent to an even function that is continuously differentiable on $[0, b]$. Equation (7 *b*) is now reconsidered in this light. Being complemented by the conditions (2), the differential operator on the left-hand side can be inverted, thus

$$f_1 = \omega_1^2[(g + \gamma\alpha^2) I - \gamma D^2]^{-1} \circ Bf_1; \tag{27}$$

and it is well known that, like A introduced earlier, this inverse can be represented as an integral operator whose kernel is piecewise continuously differentiable on

$$[0, b] \times [0, b]$$

(see appendix A). Hence an integration by parts shows that this operator is continuous $C^1 \to C^2$. It follows that $f_1 \in C^2$ and therefore (7) is satisfied pointwise.

Note that, although f_1 vanishes at $x = 0, b$, its second derivative does not. Thus the attribution $f_1 \in \hat{H}^2$ established in the course of the existence theory is the highest possible in the spaces $\hat{H}^s$ for integer s. Since f' is discontinuous at $x = 0, b$ if f is extended as an equivalent even function, the attribution $f_1 \in \bar{H}^1$ is the highest in the spaces $\bar{H}^s$. The half-range sine series representing f_1, the leading terms of which may be found by the Rayleigh–Ritz method or otherwise, therefore converges more rapidly than the half-range cosine series (in fact, for some $\delta > 0$, the sine coefficients $a_n = O(n^{-\frac{5}{2}-\delta})$ and the cosine coefficients $A_m = O(m^{-\frac{3}{2}-\delta})$ as $n, m \to \infty$). All these conclusions apply also to the higher eigensolutions f_k.

Explicit representation of $B: \hat{H}^1 \to \hat{H}^0$. This is needed if, in applying the Rayleigh–Ritz method to obtain close estimates of eigenvalues, advantage is to be taken of the comparatively rapid convergence of the odd Fourier series for solutions. Supposing $u(x)$

to be expressible by the series (24), we find the coefficients $A_m = 2\epsilon_m(u, \cos m\beta x)_0$ of the corresponding half-range cosine series. A simple calculation shows that

$$A_m = \frac{4\epsilon_m}{\pi} \sum_{n=1}^{\infty} \mathbb{C}_{nm} a_n, \tag{28}$$

where
$$\mathbb{C}_{nm} = n/(n^2 - m^2) \quad \text{if} \quad n+m \quad \text{is odd,}$$
$$= 0 \quad \text{if} \quad n+m \quad \text{is even.}$$

It is similarly found that

$$a_n = 2(u, \sin n\beta x)_0 = \frac{4}{\pi} \sum_{m=0}^{\infty} \mathbb{C}_{nm} A_m. \tag{29}$$

The representation of B as an operation on functions expressible as half-range sine series can now be deduced from (13), (28) and (29). We obtain

$$Bu = \sum_{n=1}^{\infty} b_n \sin n\beta x$$

with
$$b_n = \frac{16}{\pi^2} \sum_{m=1}^{\infty} \sum_{p=1}^{\infty} \epsilon_m \mu_m \mathbb{C}_{nm} \mathbb{C}_{pm} a_p. \tag{30}$$

Hence the quadratic functional $F(u) = (u, Bu)_0$ introduced in (21) is representable in the form

$$F(u) = \frac{1}{2} \sum_{n=1}^{\infty} a_n b_n$$
$$= \frac{8}{\pi^2} \sum_{n=1}^{\infty} \sum_{m=0}^{\infty} \sum_{p=1}^{\infty} \epsilon_m \mu_m \mathbb{C}_{nm} \mathbb{C}_{pm} a_n a_p. \tag{31}$$

In view of (20) and (21), the lowest possible value of ω^2 for a given α^2 is

$$\omega_1^2 = \min \{G(u)/F(u)\}, \tag{32}$$

where
$$G(u) = \frac{1}{b} \int_0^b \{(g + \gamma\alpha^2) u^2 + \gamma u'^2\} \, dx$$
$$= \frac{1}{2} \sum_{n=1}^{\infty} \{(g + \gamma\alpha^2) + \gamma n^2 \beta^2\} a_n^2. \tag{33}$$

The sequences $\{a_n\}$ competing for the minimum in (32) are the half-range sine coefficients for elements of $\hat{H}^1$, and (19) shows them to be just those sequences for which the series (33) converges.

We have already seen that $Bu \in \hat{H}^0$ if $u \in \hat{H}^1$, or even if merely $u \in \hat{H}^0$. This implies that the sequence $\{b_n\}$ given by (30) belong to l^2 if $\{a_n\}$ does so, and that the triple series (31) then converges.

Symmetry properties of eigensolutions. Suppose that $u(x)$ is not null but its half-range sine coefficients $a_n = 0$ for n even (respectively odd). In this case, (28) shows that $A_m = 0$ for m odd (respectively even), and (30) shows that $b_n = 0$ for n even (respectively odd). Thus, if u is either an even or odd function of $x - \frac{1}{2}b$ (i.e. is symmetric or antisymmetric about the centre-line of the channel), its image Bu has the same respective property. Symmetry preservation in this sense is evidently provided also by the differential operator on the left-hand of (7), and by its inverse appearing in (27).

It follows that every eigensolution f_k is either symmetric or antisymmetric about the centre-line, having a half-range sine expansion with only odd-order or only even-order terms. Because it is a non-negative continuous function, f_1 must therefore be in the first category of symmetry.

2.5. *Estimates for eigenvalues*

Rigorous lower bounds for λ_1 can be obtained from (21) by substituting appropriate functions which satisfy the edge conditions (2). This is the same as estimating ω_1^2 from above by use of (32). According to Rayleigh's principle, good approximations may be made quite simply by this means.

(A) As a first try, let us take $u = \sin\beta x$, which simulates the first eigensolution in being positive on $]0, b[$ and symmetric about $x = \frac{1}{2}b$. Then (33) gives immediately

$$G(u) = \tfrac{1}{2}\{g+\gamma(\alpha^2+\beta^2)\},$$

and the expression (31) reduces to

$$\begin{aligned} F(u) &= \frac{8}{\pi^2}\sum_{m=0}^{\infty}\frac{\epsilon_m \mu_{2m}}{(1-4m^2)^2} \\ &> \frac{4}{\pi^2}\left\{\frac{\coth\alpha h}{\alpha}+2\sum_{m=1}^{\infty}\frac{1}{(1-4m^2)^2(\alpha^2+4m^2\beta^2)^{\frac{1}{2}}}\right\} \end{aligned}$$

since $\coth k_{2m}h > 1$. The replacement of $\coth k_{2m}h$ by 1 for $m \geqslant 1$ has negligible effect in the case $h/b > 1$, which applies to our experimental results. We also have

$$\frac{2}{(\alpha^2+4m^2\beta^2)^{\frac{1}{2}}} > \frac{1}{m\beta}\left(1-\frac{\alpha^2}{8m^2\beta^2}\right), \tag{34}$$

and

$$\sum_{m=1}^{\infty}\frac{1}{m(4m^2-1)^2} = \tfrac{3}{2}-2\ln 2 = 0{\cdot}1137,$$

$$\frac{1}{8}\sum_{m=1}^{\infty}\frac{1}{m^3(4m^2-1)^2} = 0{\cdot}01396.$$

Hence

$$F(u) > \frac{4}{\pi^2}\left(\frac{\coth\alpha h}{\alpha}+\frac{0{\cdot}1137}{\beta}-\frac{0{\cdot}01396\alpha^2}{\beta^3}\right), \tag{35}$$

and this is a useful estimate provided $h > b$ and α^2/β^2 is substantially smaller than 8. It follows according to (32) that

$$\omega_1^2 < \frac{\pi^2\alpha\{g+\gamma(\alpha^2+\beta^2)\}}{8\{\coth\alpha h+0{\cdot}1137(\alpha/\beta)-0{\cdot}01396(\alpha/\beta)^3\}}, \tag{36}$$

and the right-hand side of (36) can be expected to give a fair approximation to ω_1^2 particularly when $h > b$ and α/β is small.

We note that for α/β small the dispersive properties of the first wave mode according to the estimate (36) are akin to those of the first mode for the simplified problem discussed in §2.2. Thus $\omega_1^2(\alpha)$ is comparable with $\tilde{\omega}_0^2(\alpha)$. The wave with frequency ω_1 behaves in effect as if g in the simplified problem were replaced by $g' = \frac{1}{8}\pi^2(g+\gamma\beta^2)$, and in the long-wave limit $\alpha \to 0$ its phase velocity and group velocity equal $(g'h)^{\frac{1}{2}}$. For water with $\gamma = 72$ mN/m, we have $g' > 4g$ if $b < 5{\cdot}7$ mm approximately, so that in this case the effect of the edge constraints more than doubles the long-wave velocity of the fundamental mode.

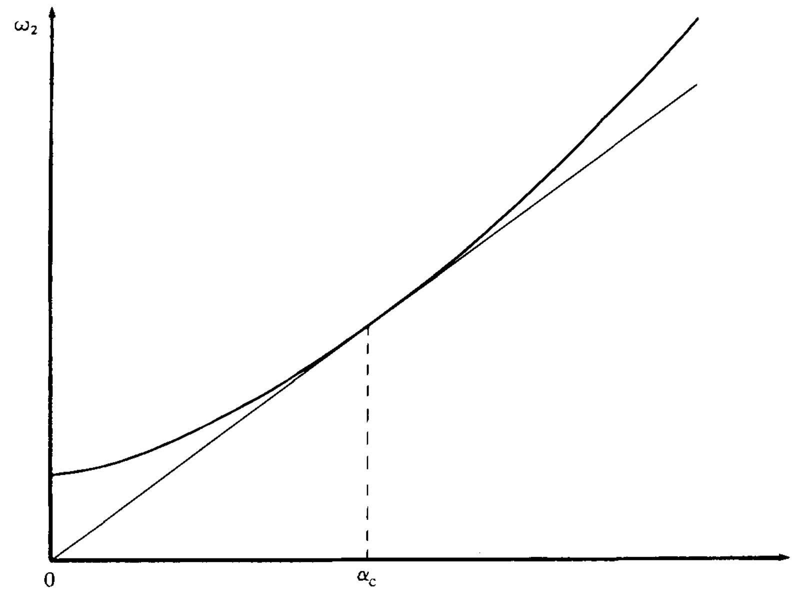

FIGURE 2. Dispersion relation for the second wave mode, illustrating the minimum of phase and group velocities.

(*B*) We may presume that the second eigensolution f_2 is antisymmetric about $x = \frac{1}{2}b$. Hence an estimate for ω_2^2 is obtained by considering the test function $\sin 2\beta x$, which obviously satisfies the requisite condition of orthogonality with the symmetric eigensolution f_1. On the replacement of $\coth k_1 h > 1$ by 1 in the estimate for F, it is thus established that

$$\omega_2^2 < (\pi^2/64\iota)(\alpha^2+\beta^2)^{\frac{1}{2}}\{g+\gamma(\alpha^2+4\beta^2)\}, \tag{37}$$

where
$$\iota = \sum_{m=1}^{\infty} \frac{1}{(4m^2-4m-3)^2(2m-1)} = 0{\cdot}125.$$

Unlike $\omega_1^2(\alpha)$ and in keeping with the estimate (37), $\omega_2^2(\alpha)$ clearly must have a positive limit as $\alpha \to 0$; for $\omega_2(0)$ can be interpreted as the lowest possible frequency of two-dimensional standing waves that are independent of the co-ordinate z along the channel. For such waves the condition

$$\int_0^b f(x)\,dx = 0 \tag{38}$$

is required by conservation of the liquid mass, thus excluding f_1 as a possible mode but being automatically satisfied when f is antisymmetric about $x = \frac{1}{2}b$. Since the phase velocity $c_2 = \omega_2/\alpha$ is unbounded as $\alpha \to 0$, it may be expected to have a minimum at some positive value of $|\alpha|$, say a_c. This result is illustrated in figure 2, which is drawn from (37). The figure makes plain that the group velocity $d\omega_2/d\alpha$ is less than c_2 for $0 < \alpha < \alpha_c$ and greater for $\alpha > \alpha_c$. A physical implication thus provided, recalling one that is well known regarding the simplified problem of §2.2, is that localized applied-force systems moving along the channel at constant speed U may generate steadily lengthening wave-trains in the second mode if $U > c_2(\alpha_c)$, but cannot do so if

$$U < c_2(\alpha_c).$$

Waves with $\alpha > \alpha_c$ will appear ahead since their group velocity exceeds $c_2(\alpha) = U$ and waves with $0 < \alpha < \alpha_c$ will appear behind. Being an absolute minimum with respect to α, the (positive) frequency $\omega_2(0)$ is physically significant as the 'cut-off' frequency for the second mode. When excited at any lower frequency, waves in this mode will not propagate along the channel.

The preceding considerations apply also to the third mode, which may be presumed to have the same form of symmetry as the first. The condition (38) is satisfied by f_3 in the limit $\alpha \to 0$, being presented analytically as the limiting form of the orthogonality condition that holds between f_1 and f_3 for non-zero α. The latter is equivalent to $(f_1, Bf_3)_0 = 0$, which is the same as

$$\sum_{m=0}^{\infty} \mu_{2m} A_{2m}^{(1)} A_{2m}^{(3)} = 0, \tag{39}$$

where $A_{2m}^{(1)}$ and $A_{2m}^{(3)}$ are the half-range cosine coefficients for f_1 and f_3. We have

$$\mu_0(\alpha) = \alpha^{-1} \coth \alpha h = O(1/\alpha^2 h) \quad \text{as} \quad \alpha \to 0,$$

and $\mu_{2m}(0) = (\coth 2m\beta)/2m\beta$ for $m \geqslant 1$. Since $A_0^{(1)}$ is not zero, (39) implies that $A_0^{(3)} = 0$ in the limit $\alpha \to 0$, and this condition is the same as (38) for f_3.

It has a particular bearing on the experiments to estimate the cut-off frequency $\omega_3(0)$, which may be interpreted as the lowest possible frequency of two-dimensional standing waves that are symmetric about $x = \frac{1}{2}b$. Writing F_0 and G_0 for the functionals (31) and (33) in the case $\alpha = 0$, we have that $\omega_3^2(0)$ is the minimum of $G_0(u)/F_0(u)$, where u ranges over those elements of $\hat{H}^1$ that are symmetric and satisfy (38). An estimate from above is thus given by taking

$$u = \tfrac{1}{3} \sin \beta x - \sin 3\beta x,$$

which satisfies all the conditions; and according to Rayleigh's principle it may be expected that this estimate too is fairly close. We obtain immediately

$$G_0(u) = \tfrac{1}{9}(5g + 41\gamma\beta^2),$$

and after some reduction

$$\begin{aligned} F_0(u) &> \frac{4096}{9\pi^2\beta} \sum_{m=1}^{\infty} \frac{m^3}{(4m^2-1)^2(4m^2-9)^2} \\ &= 0{\cdot}076448b. \end{aligned}$$

Here inequality arises only through replacing $\coth 2m\beta h$ by 1, which makes negligible difference in respect of our experimental values. It follows that

$$\omega_3^2(0) < 7{\cdot}267(g/b) + 588{\cdot}1(\gamma/b^3). \tag{40}$$

(C) The test function $\sin \beta x$ chosen in (A) above is unlike the eigensolution f_1 in that its second derivative vanishes at $x = 0, b$. To examine the sensitivity of the estimate to this feature, let us try

$$u = (x/b)\{(1-(x/b)\} \tag{41a}$$

$$= \frac{1}{6} - \frac{1}{\pi^2} \sum_{m=1}^{\infty} \frac{\cos 2m\beta x}{m^2}, \tag{41b}$$

for which u'' is a constant on $]0, b[$ but, according to the representation (41*b*) of u as a half-range cosine series, u'' does not exist at $x = 0, b$ (i.e. u' has a saltus at each of these points). From (41*a*) we readily obtain

$$G(u) = \tfrac{1}{30}(g+\gamma\alpha^2)+\tfrac{1}{3}\gamma/b^2,$$

and from (41*b*), making use of (13),

$$F(u) = \frac{\mu_0}{36}+\frac{1}{2\pi^4}\sum_{m=1}^{\infty}\frac{\mu_{2m}}{m^4}.$$

The use again of (34) now gives

$$F(u) > \frac{\coth\alpha h}{36\alpha}+\frac{1}{4\pi^2\beta}\left\{\sum_{m=1}^{\infty}\frac{1}{m^5}-\frac{\alpha^2}{8\beta^2}\sum_{m=1}^{\infty}\frac{1}{m^7}\right\},$$

in which the sums of the two infinite series are respectively

$$\zeta(5) = 1\cdot0369 \quad\text{and}\quad \zeta(7) = 1\cdot0083.$$

It follows that
$$\omega_1^2 < \frac{\alpha\{(6/5)(g+\gamma\alpha^2)+12(\gamma/b^2)\}}{\coth\alpha h+0\cdot09581(\alpha/\beta)-0\cdot01165(\alpha/\beta)^3}. \tag{42}$$

For small α/β, this estimate is slightly less, and thus better, than (36). Comparing coefficients in the respective numerators and recalling that $\beta = \pi/b$, we find

$$\tfrac{6}{5} < \pi^2/8 = 1\cdot234 \quad\text{and}\quad 12 < \pi^4/8 = 12\cdot18.$$

The closeness of these figures, notwithstanding the gross difference in the curvature properties of the respective test functions around $x = 0, b$, is reason for confidence in the estimates.

(*D*) It was explained at the end of § 2.4 that the half-range sine series for f_1 consists of odd-order terms only. Accordingly, to estimate ω_1^2 by the Rayleigh–Ritz method, a truncated series of this form may be substituted in the quotient on the right-hand side of (32) and a minimum found by varying the coefficients of the series. Here we take only two terms; and since the minimum is plainly not achieved when the coefficient of the leading term $\sin\beta x$ is zero, we may consider

$$u_R = \sin\beta x+R\sin 3\beta x,$$

finding the minimum with respect to the number R. Then (33) gives

$$G(u_R) = \tfrac{1}{2}[g+\gamma(\alpha^2+\beta^2)+\{g+\gamma(\alpha^2+9\beta^2)\}R^2],$$

and (31) gives

$$F(u_R) = \frac{8}{\pi^2}\sum_{m=0}^{\infty}\epsilon_m\mu_{2m}\left\{\frac{1}{(4m^2-1)^2}+\frac{6R}{(4m^2-1)(4m^2-9)}+\frac{9R^2}{(4m^2-9)^2}\right\}. \tag{43}$$

A lower bound for the sum of the terms independent of R in (43) is provided by (35). A lower bound for the sum of the terms in R^2 is similarly found to be

$$\frac{4}{\pi^2}\left\{\frac{\coth\alpha h}{9\alpha}+\frac{0\cdot4570}{\beta}-\frac{0\cdot04793\alpha^2}{\beta^3}\right\}R^2. \tag{44}$$

The first two terms in R are

$$\frac{4}{\pi^2}\left\{\frac{2\coth\alpha h}{3\alpha}-\frac{4\coth[(\alpha^2+4\beta^2)^{\frac{1}{2}}h]}{5(\alpha^2+4\beta^2)^{\frac{1}{2}}}\right\}R, \tag{45}$$

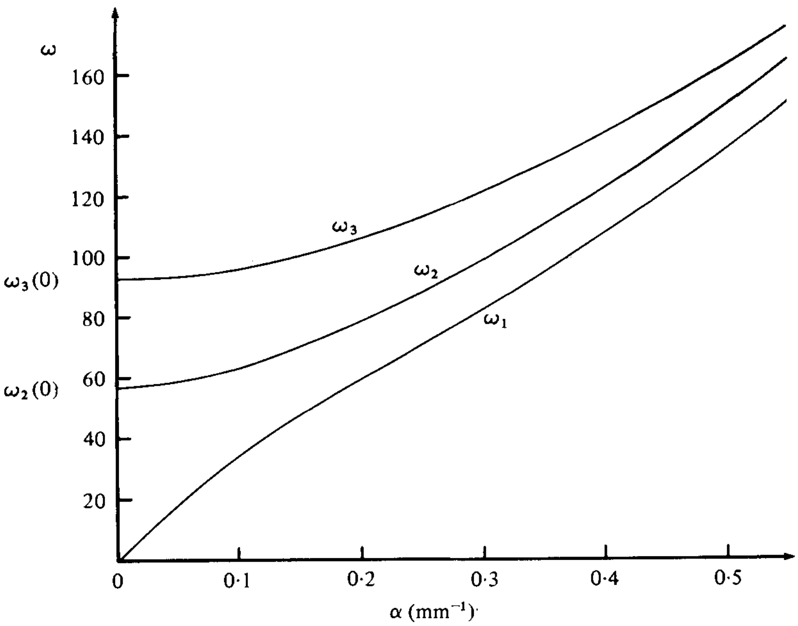

FIGURE 3. Dispersion relations for the first three wave modes, calculated for $b = 20{\cdot}29$ mm, $h = 21{\cdot}5$ mm, $\gamma = 72$ mN/m.

and the remaining terms are positive. It may be seen that if $\alpha^2 < (100/11)\beta^2$, as will now be assumed, the number expressed within the braces in (45) is positive, and therefore the minimum of $G(u_R)/F(u_R)$ is achieved by a positive value of R. A lower bound for the sum of the remaining terms may accordingly be found by use of (34), and the result is

$$\frac{4}{\pi^2}\left(\frac{0{\cdot}03134}{\beta}-\frac{0{\cdot}00925\alpha^2}{\beta^3}\right)R. \tag{46}$$

The required lower bound for $F(u_R)$ is the sum of the right-hand side of (35), (44), (45) and (46), being a quadratic form in R. The results of minimizing the quotient of $G(u_R)$ and this bound, so estimating ω_1^2, will be presented numerically in figure 4.

3. Experiments

The theory presented in §2 has shown that for a given positive wavenumber α ($= 2\pi/\lambda$, where λ is wavelength), there exists an infinite sequence of wave modes f_k ($k = 1, 2, \ldots$) whose frequencies form an ascending sequence $0 < \omega_1(\alpha) < \omega_2(\alpha) \leqslant \ldots$. The situation is illustrated in figure 3, which highlights that the first mode alone has the property $\omega_1(\alpha) \to 0$ as $\alpha \to 0$. For $k > 1$, the $\omega_k(\alpha)$ have positive limits as $\alpha \to 0$. In the experiments, travelling waves of the class in question were generated by a vibrating bar at one end of a uniform channel, so that frequency ω rather than α was the parameter under control. The modes capable of being thus excited as travelling waves are indicated in figure 3 by the intersections of a line $\omega =$ constant with the curves $\omega = \omega_k(\alpha)$; and since the wave-maker was mounted symmetrically across the channel, only the modes $k = 1, 3, 5, \ldots$ are relevant.

These considerations establish an important point of interpretation regarding the experimental measurements. For the three channels used, which are detailed in §3.1 below, the estimate (40) of the cut-off frequency $\omega_3(0)$ gives respectively (*a*) 67·9 ms, (*b*) 30·6 ms and (*c*) 10·4 ms for the critical period $T_c = 2\pi/\omega_3(0)$. These values are smaller than values of the wave period in the experiments, and it can therefore be concluded that only the first mode was excited.

3.1. *Apparatus*

Common difficulties have to be met in conducting experiments with liquids whose surface tension is required to be constant and to be accurately known. In particular, there is a need to moderate the reduction in surface tension and the dilatational elasticity of the surface that arise from the presence of even minute quantities of surface-active substances. Water and mercury, for example, are both particularly convenient in that the properties of the pure liquid are well established, but both are highly prone to contamination by common organic materials. Water was used in the present experiments, having the advantage that it is easier to clean and, when prepared in plenty, can be thrown away on becoming contaminated. The water to be used was distilled twice: first, to remove inorganic salts, by a continuously running, all Pyrex/silica, 3 kW still; second, in 8 l batches, by an all Pyrex, 10 l closed system. The purity of the water was tested by observing air bubbles entrained by shaking: samples allowing bubbles to persist for as long as 0·5 s at the surface were rejected.

The need to avoid contamination also restricts the choice of solid materials for apparatus. Good materials in this respect include PTFE (polytetrafluoroethylene, or Teflon), Pyrex glass and stainless steel, which can be efficiently cleaned both by scrubbing and with strong chromic acid. These are otherwise inexpedient for experiments such as ours, however, and we decided to use Perspex, a comparatively inexpensive and easily workable material. Although Perspex cannot be treated with chromic acid or other powerful cleansing agents, many previous experiments had shown that it can be well cleaned by gentle scrubbing with detergent and then thorough rinsing with the clean water whose preparation is described above.

Two methods were used to construct narrow channels as required for the experiments. First, they were assembled from long strips of Perspex, but the necessary use of solvent cement was seen to produce residual stresses liable to put the finished channel out of true. The second and finally preferred method was to mill the channels out of a solid block of Perspex.

Each channel was fitted with a beach at one end to absorb the wave energy. The beaches were all made from a single, wide block of Perspex milled to the required profile. The flat part of the beach, 400 mm long, had a slope about 2 %, and joined smoothly to a short curved section about 50 mm long with a radius of curvature of 80 mm. No reflexion was observable from the beaches in any of the channels over the range of wavelengths covered in these experiments. As water has a finite contact angle on Perspex, the water surface would normally form a significant meniscus, sufficient to give a measurable reflexion, on such a gently sloping beach. This effect was avoided by terminating the beach against a vertical wall, such that the depth of water at the wall was about 0·5 mm. A glass rod was used to draw the water up the beach to this wall, at which the water would then stay fixed. The depth profile on the beach was thereafter very efficient for wave damping. The channels all had 1 m of working length between the wave generator and the start of the beach. Three channels were used in the experiments reported here: (*a*) width $b = 20{\cdot}3$ mm, depth $h = 21{\cdot}5$ mm; (*b*) $b = 10{\cdot}6$ mm, $h = 20{\cdot}0$ mm; (*c*) $b = 4{\cdot}0$ mm, $h = 25{\cdot}0$ mm.

The wave generator in each channel was a bar of PTFE of rectangular section, cut to a loose fit spanning one end of the channel. One end of each bar was tapped to take a 2 BA bolt, which fixed it to a small electrodynamic vibrator (Ling–Altec). Each bar executed nearly horizontal oscillations along the channel, the vibrator being driven through a power amplifier from an electronic oscillator with continuously variable frequency.

3.2. *Setting up*

Each channel was arranged horizontally on a levelling table, and the levelling was done with the channel full of water. The free surface was required to be everywhere horizontal, touching the top edges of the channel, and this condition could easily be judged by observing reflexions of fluorescent light fittings on the laboratory ceiling. When the surface was exactly flat, the reflected image showed no distortion, and by suitable positioning of the light source and observer it could be arranged that the passage of a wave along the channel caused an oscillation of the reflected image such that a distortion in one direction was followed a half-period later by an identical distortion in the opposite direction. The channels were levelled by successively checking the condition of flatness of the surface at both ends of the working section. This was found to be a more sensitive test than the use of a spirit level.

Once set up, the apparatus was thoroughly cleaned by use of a soft sponge and detergent, being then rinsed with a jet of hot tap water before a final rinse with the clean distilled water. The channel and the prepared water were allowed to reach room temperature before filling, which was done with a series of Pyrex-glass pipettes cleaned by chromic acid. Between experimental runs, the water was changed by sucking out the existing charge with a clean glass capillary connected to a jet pump.

3.3. *Measurements*

The wave period was measured by means of an electronic timer which averaged over 10 cycles. Expected precision was better than $0{\cdot}5\,\%$. Waves in the channel were monitored by means of a capacitance-probe system (Wayne–Kerr), which responded to changes in the capacitance between the sensing area of the probe, fixed horizontally, and the heaving water surface at a small distance beneath. Due to the comparatively small widths of the channels and to the varying spanwise curvature of the surface during passage of the waves, precise measurements of wave amplitude could not be made by this means. By visual observation, however, it was confirmed that the peak-to-peak displacement amplitude at the channel centre was always less than 1 mm, usually much less.

To measure the wavelength of a progressive wave train at fixed frequency, the probe was moved gradually along the channel and the phase of the probe output was compared with that of the oscillator driving the wavemaker. Horizontal position of the probe being measured from a brass metre scale, to within $\pm\,0{\cdot}5$ mm, the wavelength was found as an integral fraction of the distance between stations of phase coincidence, which were located by observing Lissajous figures formed on an oscilloscope from the two signals. In each case, the two most carefully measured stations of phase coincidence were separated by as many (counted) wavelengths as possible. Precision better

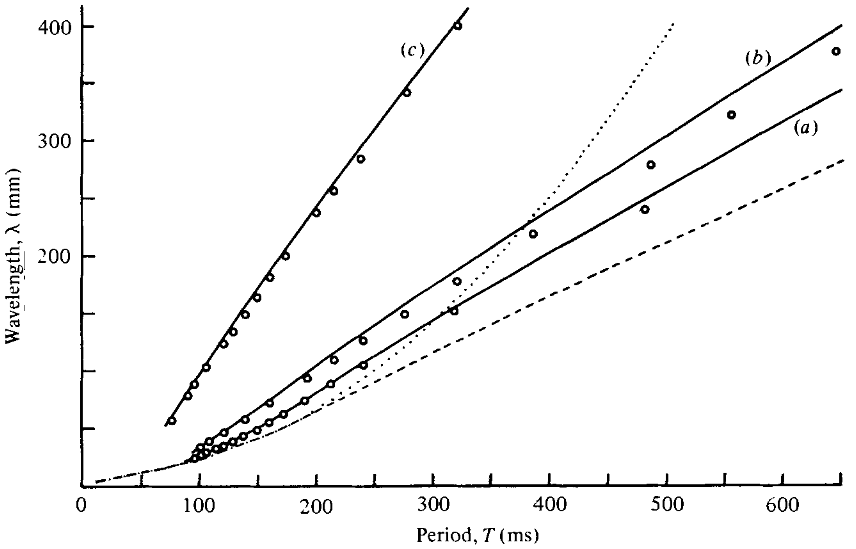

FIGURE 4. Comparison of theoretical curves and experimental points for the three channels: (*a*) $b = 20{\cdot}3$ mm, $h = 21{\cdot}5$ mm; (*b*) $b = 10{\cdot}6$ mm, $h = 20{\cdot}0$ mm; and (*c*) $b = 4{\cdot}0$ mm, $h = 25{\cdot}0$ mm. ⋯, theoretical curve for long-crested deep-water waves; ---, theoretical curve for long-crested shallow-water waves, equation (10), for $h = 20{\cdot}0$ mm. All results assume $\gamma = 72{\cdot}0$ mN/m.

than $\pm 1\,\%$ was estimated for all the measurements of wavelength to be reported here.

Because of the small widths of the channels, the surface tension of the water could not be measured *in situ*. The expedient adopted for all three, channels was to assume that, by repeated removal by suction and replenishment of the water, any residual contamination would be reduced to insignificance, so that measurements of surface tension made (on the supply of clean water) immediately after refilling would tend eventually to represent a clean surface in the channel. At the end of each experimental run, earlier measurements of wave properties were repeated in order to establish that the surface tension had not changed significantly during the run.

3.4. *Experimental results*

For the three channels (*a*), (*b*) and (*c*) whose widths and depths are specified in § 3.1, measured values of wavelength and period are presented in figure 4. The figure also shows theoretical curves, for the respective b and h, according to the second-order Rayleigh–Ritz estimate explained in § 2.5 *D*. For comparison, two further theoretical curves are included according to the well-known formula (10) with $m = 0$ (i.e. for long-crested waves free from edge constraints). A satisfactory agreement is apparent between the measurements and the present theoretical predictions, while their disparity with the properties of long-crested waves is plainly demonstrated.

Respective to the two wider channels (*a*) and (*b*), the final estimate of $\omega_1(\alpha)$ in § 2.5 *D* was found to be significantly closer to experiment than the simpler estimates presented as the inequalities (36) and (42) in §§ 2.5 *A* and *C*. Since it may be of interest to compare these estimates as successive improvements in the method of approximate

α (mm^{-1})	ω_1 (s^{-1})			
	Equation (36)	Equation (42)	R-R	Experimental
0·02	10·72	10·59	10·48	10·28
0·04	19·81	19·60	19·42	19·06
0·06	26·89	26·69	26·46	26·09
0·08	32·47	32·39	32·05	31·53
0·10	37·12	37·32	36·73	36·19

TABLE 1. Calculated and experimental values of $\omega_1(\alpha)$ for channel (a): $b = 20{\cdot}29$ mm, $h = 21{\cdot}50$ mm. The fourth column gives values according to the Rayleigh–Ritz estimate explained in §2.5 D.

solution, some calculated values of $\omega_1(\alpha)$ respective to channel (a) are given in table 1, which includes interpolated or extrapolated experimental values. For the narrowest channel (c), the estimate (42) was found to be within 2 % in excess of the experimental values, being close to, but not bettered by, the second-order estimate.

As shown by figure 4 and by the last two columns of table 1, the difference between theory and experiment is quite small but has a definite trend. It appears that the waves in practice were slightly slower than predicted. This discrepancy is in the direction such that it may be accountable to the residual error in the approximation to $\omega_1(\alpha)$, which the complete theory shows to be inevitably an overestimate; and presumably the discrepancy would be reduced by closer approximations to the exact theoretical value of $\omega_1(\alpha)$ specified by (32). Other possible explanations for the small discrepancy can be recognized, however, and in view of these we have considered it hardly warranted to complete the somewhat formidable task of taking the Rayleigh–Ritz method of approximation to further stages. One of the possibilities in view is that boundary layers in the channels reduced the effective depths. Another is that residual contamination reduced the surface tension of the water. Although the stringent procedures described in §§3.1 and 3.2 were consistently followed, so that purity of the water in the experiments was fairly well assured, it was not possible to measure its surface tension *in situ* and therefore some uncertainty about this factor must remain.

4. Conclusion

We have described a class of water waves whose properties, unlike those of the more familiar, long-crested waves observable in comparatively wide channels, depend principally on surface tension and the span of the channel in which the waves propagate. Attention has been focused on a model situation, the brimful rectangular channel, where the condition supposed to hold at each edge of the free surface plainly accords with the experimental facts. Returning to a point discussed in §1, however, we may additionally claim for this condition that it is often the relevant one even in the absence of a sharp corner to locate the contact line. Thus, particularly on a clean solid surface, contact-angle hysteresis is often sufficient to immobilize the contact line against the action of waves whose amplitude is fairly small. Although it appears that until now little note has been made of capillary phenomena determined in this manner, they are not uncommon in water-wave experiments, being noticeable in channels with widths as much as 100 mm or more – that is, considerably wider than channels such as used by us, in which the influence of the edge constraints is predominant. By dealing in depth with the model situation, for which the theory can be taken to particularly straightforward and good estimates of measurable properties, this investigation at least opens the record of a promising variety of water-wave phenomena. Evidently much remains to be done. For example, the three variants of the present problem that are reviewed theoretically in appendix B are open to numerical and experimental study.

We gratefully acknowledge support given by the Natural Environment Research Council to the programme of research, on surface-tension effects, of which this investigation has been part. We are also indebted to Mr J. K. Bartington and Mr J. E. Davis, Technical Assistants in the Fluid Mechanics Research Institute, for expert help in the design and construction of the apparatus.

Appendix A. Simplicity of the first eigenvalue

We reconsider the eigenvalue problem in the form (27), rewriting the equation as

$$\lambda_1 f_1 = \mathscr{C} f_1, \tag{A 1}$$

where the operator

$$\mathscr{C} = [(g+\gamma\alpha^2)I - \gamma D^2]^{-1} \circ B \tag{A 2}$$

has been seen to possess the same general properties as $\mathscr{B}$ introduced above (24). In particular, $\mathscr{C}$ is completely continuous $\hat{H}^1 \to \hat{H}^1$. A further property to be used here is that $\mathscr{C}$ maps the cone

$$K = \{v \in \hat{H}^1 : v \geqslant 0 \text{ (a.e) on } [0,1]\}$$

into itself. The cone K is reproducing (generating): that is, every element of $\hat{H}^1$ can be represented in the form $v = v_+ - v_-$, where $v_+, v_- \in K$. [For the argument needed to verify this fact, see Stampacchia (1963).]

It was recognized in § 2.4 that the first eigensolution f_1 is non-negative, being thus an element of K. A concomitant fact now to be demonstrated is that the eigenvalue λ_1 is simple. This means that f_1 is the unique non-zero solution of the equations

$$(\mathscr{C} - \lambda_1 I)^n f = 0 \quad (n = 1, 2, \ldots).$$

The positivity of $\mathscr{C}$ with respect to the cone K is implied by properties of the two operators from which $\mathscr{C}$ is composed according to (A 2). It was proved at the end of § 2.3 that Bv is a non-negative element of $\bar{H}^0$ if $v \in K$. The second operator, which is completely continuous $\bar{H}^0 \to \hat{H}^1$, evidently takes any such element of $\bar{H}^0$ into an element of K, for it can be represented as an integral operator whose kernel is positive on $]0,b[\times]0,b[$. Specifically, we have

$$[(g+\gamma\alpha^2)I - \gamma D^2]^{-1} v(x) = \frac{1}{\gamma}\int_0^b k(x,s)\,v(s)\,ds, \tag{A 3}$$

in which

$$k(x,s) = \frac{\sinh\kappa x\,.\,\sinh\kappa(b-s)}{\kappa\sinh\kappa b} \quad \text{if} \quad 0 \leqslant x \leqslant s,$$

$$= k(s,x) \quad \text{if} \quad s \leqslant x \leqslant b,$$

with

$$\kappa = \{\alpha^2 + (g/\gamma)\}^{\frac{1}{2}}.$$

It is found that $$\int_0^b k(x,s)\,ds = \frac{2\sinh\frac{1}{2}\kappa x\,.\sinh\frac{1}{2}\kappa(b-x)}{\kappa^2\cosh\frac{1}{2}\kappa b},$$

which function belonging to K will be denoted by u_0. We shall show that $\mathscr{C}$ is u_0-*positive* (cf. Krasnosel'skii 1964, chap. 2), by which we mean that, for every non-zero $v\in K$, positive numbers σ and τ can be found such that

$$\sigma u_0 \leqslant \mathscr{C}u \leqslant \tau u_0. \tag{A 4}$$

Here the symbol $\leqslant$ connotes ordering with respect to the cone K, but it will also be used in other senses that are obvious from their context.

To establish that $\mathscr{C}$ is u_0-bounded from above, the standard inequality

$$\operatorname{ess\,sup} v \leqslant 2^{-\frac{1}{2}}\|v\|_1$$

may be coupled with the fact that $B(1) = \mu_0$ [cf. (13)]. It follows at once from (A 2) and (A 3) that τ in (A 4) can be assigned the value $\mu_0\|v\|_1/2^{\frac{1}{2}}\gamma$.

To verify the u_0-boundedness of $\mathscr{C}$ from below, consider any particular non-zero $v\in K$, thus $v \geqslant 0$ (a.e.) on $[0,\ b]$ and $v \not\equiv 0$. Since v is equivalent to a continuous function, v is then positive on a sub-interval $[x_1, x_2]$ of $[0,b]$ with $x_2 > x_1$. But, according to the conclusion stated in the final paragraph of § 2.3, Bv is positive where v is positive. Hence a number $\epsilon > 0$ can be found such that $Bv(x) \geqslant \epsilon\ \forall\, x\in[x_1,x_2]$, and we also know from the end of § 2.3 that $Bv(x) \geqslant 0\ \forall\, x\in[0,b]$. Dealing separately with the three, possibly distinct cases $0 \leqslant x \leqslant x_1$, $x_1 \leqslant x \leqslant x_2$ and $x_2 \leqslant x \leqslant b$, a straightforward calculation shows that, $\forall\, x\in[0,b]$,

$$\int_{x_1}^{x_2} k(x,s)\,ds \geqslant u_0(x)\,.\tfrac{1}{4}\operatorname{cosech}^2(\tfrac{1}{2}\kappa b)\,.\kappa^2(x_2-x_1)\min\{(x_1+x_2),(2b-x_1-x_2)\}. \tag{A 5}$$

It now follows from (A 2) and (A 3) that σ in (A 4) can be assigned the value ϵ/γ times the positive coefficient of $u_0(x)$ on the right-hand side of (A 5).

Having confirmed that $\mathscr{C}$ is a u_0-positive operator with respect to the reproducing cone K, we can apply a series of theorems proved in chapter 2 of Krasnosel'skii's monograph (1964). The conclusions thus available are as follows.

First (theorem 2.10): the eigenvalue λ_1 is simple.

Second (theorem 2.11): the normalized eigensolution f_1 is unique in K. [This fact is otherwise evident from the condition of orthogonality between f_1 and another eigensolution f_k corresponding to a different eigenvalue, thus $(f_1, Bf_k)_0 = 0$. This condition plainly cannot be satisfied if f_k is another non-zero element of K.]

Third (theorem 2.13): λ_1 is greater than any other eigenvalue. [This fact has otherwise been demonstrated in § 2.4.]

Fourth (theorem 2.5): existence of an eigensolution $f_1\in K$ is implied by the properties that $\mathscr{C}: K\to K$ is completely continuous, that $\mathscr{C}u_0 \geqslant \sigma u_0$ $(\sigma > 0)$ according to (A 4), and that $-u_0\notin K$.

With allowance for all admissible values of the parameters g, γ, b, h and α^2, nothing that is comparably definite can be said about the possibility that eigenvalues other than λ_1 are simple. We may reasonably presume, however, that *typically* all the eigenvalues are simple.

Note finally that the left-hand part of (A 4) shows f_1 to be positive on $]0,b[$.

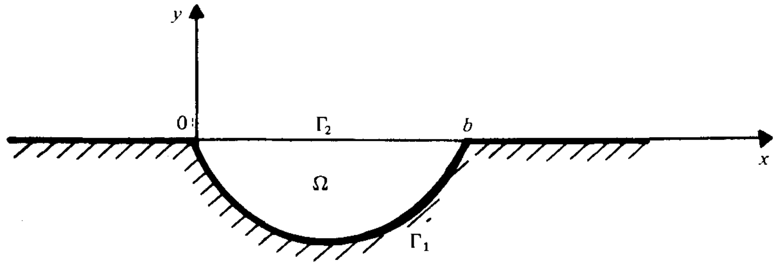

FIGURE 5. Cross-section of arbitrarily shaped channel.

Appendix B. Generalizations of theory

An advantage of the problem treated in § 2 is that an explicit representation of the operator B is available, clarifying its role and enabling eigenvalues to be estimated simply. The theory required to establish the existence of eigensolutions is not dependent on this feature, however, and may be extended readily to other physically interesting problems of the type exemplified most straightforwardly by the original problem. Here the treatment of three such problems will be outlined.

B 1. *Channel of arbitrary cross-section*

Suppose that, as illustrated in figure 5, the submerged part of the boundary of the cross-sectional domain Ω in the x, y plane is a piecewise smooth curve Γ_1, with Ω locally on one side of Γ_1, and as before the undisturbed free boundary Γ_2 is the horizontal straight line between $(0,0)$ and $(b,0)$. The equation of the perturbed free surface being again assumed to have the form (1) subject to (2), the linearized hydrodynamic problem leads as before to

$$(g+\gamma\alpha^2)f-\gamma f'' = \omega^2\Phi(x,0) = \omega^2 Bf, \tag{B 1}$$

and $\Phi(x,y)$ is now specified as the solution of the Neumann problem

$$\left.\begin{aligned} \Phi_{xx}+\Phi_{yy}-\alpha^2\Phi &= 0 \quad \text{in} \quad \Omega, \\ \partial\Phi/\partial n &= 0 \quad \text{on} \quad \Gamma_1, \\ \partial\Phi/\partial n \equiv \partial\Phi/\partial y &= f(x) \quad \text{on} \quad \Gamma_2. \end{aligned}\right\} \tag{B 2}$$

If weak eigensolutions $f \in \hat{H}^1$ are again defined as in the context of (20), the only change is the generalized specification of the Neumann problem (B 2) which determines the operator B in (B 1). For any given Ω, the weak solution $\Phi \in H^1(\Omega)$ is defined uniquely by (17), provided, as was noted below (17), that f is a distribution belonging to $H^{-\frac{1}{2}}(0,b)$. Since $\hat{H}^1 \subset H^{-\frac{1}{2}}(0,b)$, the definition (17) thus serves for the present application, establishing that

$$Bf \equiv \Phi(x,0) \in H^{\frac{1}{2}}(0,b) \subset \bar{H}^0.$$

From this attribution of Bf, the existence theory may proceed exactly as in § 2.4.

It is noteworthy that the quadratic functional $F(u) = (u, Bu)_0$, which was introduced in (21) and thereafter shown to be weakly continuous in $\hat{H}^1$, is equivalent to

$$-(2/b) \min_{\xi \in H^1(\Omega)} \mathscr{F}(\xi, u),$$

where $\mathscr{F}$ is defined below (17).

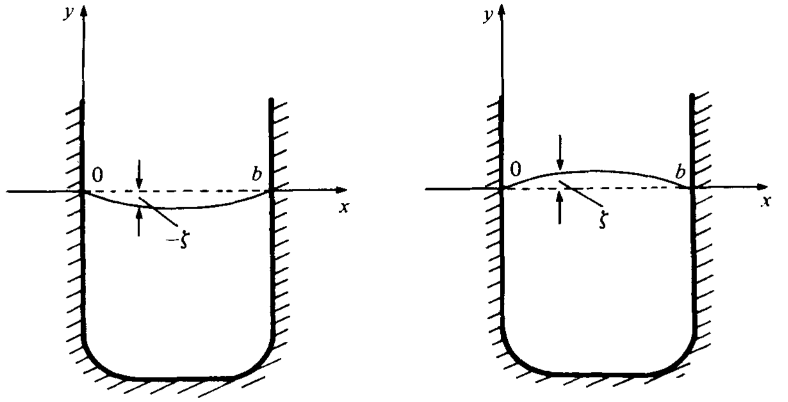

FIGURE 6. Undisturbed states of channels respectively underfilled and overfilled relative to the contact lines.

B 2. *Curved free surface*

We suppose that, while the edges of the free surface are again fixed in the horizontal lines $(x, y) = (0, 0)$ and $(b, 0)$, the undisturbed surface Γ_2 is not flat (figure 6). Let its equation be $y = \zeta(x)$ with $\zeta(0) = \zeta(b) = 0$. Then ζ is respectively negative or positive on $]0, b[$ accordingly as the channel is less than brimful or is overfilled. The curvature of Γ_2 is $\zeta'/(1+\zeta'^2)^{\frac{3}{2}}$, and according to the hydrostatic law of pressure the equation of equilibrium is therefore

$$\frac{\gamma\zeta''}{(1+\zeta'^2)^{\frac{3}{2}}} - g\zeta = \text{constant}, \tag{B 3}$$

where the constant has to be chosen so that the solution of (B 3) satisfying the edge conditions complies with the given filling of the channel. It is not easy to solve (B 3) explicitly, but the ideas in question may be illustrated very simply by supposing that $|\zeta'| \ll 1$ everywhere and accordingly using the linearized approximation to the curvature. In place of (B 3) we then have

$$\zeta'' - \kappa^2\zeta = \text{constant}, \quad \kappa^2 = g/\gamma,$$

and the constant can be chosen to provide the solution

$$\zeta = \zeta_m\left\{\frac{\cosh\frac{1}{2}\kappa b - \cosh\kappa(x-\frac{1}{2}b)}{\cosh\frac{1}{2}\kappa b - 1}\right\},$$

where $\zeta_m = \zeta(\frac{1}{2}b)$ is the largest displacement from the horizontal plane $y = 0$.

Let θ denote the angle between the tangent to Γ_2 and the horizontal: thus

$$\tan\theta = \zeta'(x),$$

where $\zeta(x)$ is the appropriate solution of (B 3), and in general $0 \leqslant |\theta| < \frac{1}{2}\pi$. If the equation of the perturbed free surface is

$$y = \zeta(x) + \eta(x, z, t) \tag{B 4}$$

and ϕ is the velocity potential, the linearized kinematical condition at the surface is

$$\eta_t \cos\theta = \partial\phi/\partial n,$$

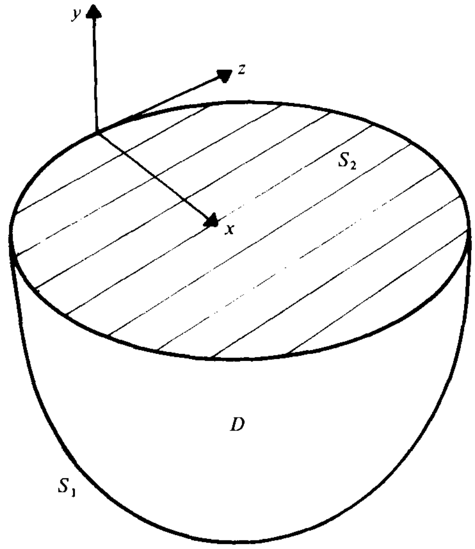

FIGURE 7. Arbitrarily shaped basin filled to the horizontal plane $y = 0$.

where the normal derivative is evaluated on Γ_2, that is, on $y = \zeta(x)$. Hence, supposing η to have the form specified in (1) and taking the appropriate form of ϕ as before, we obtain in place of (B 2)

$$\left.\begin{aligned} &\Phi_{xx}+\Phi_{yy}-\alpha^2\Phi = 0 \quad \text{in} \quad \Omega, \\ &\partial\Phi/\partial n = 0 \quad \text{on} \quad \Gamma_1, \\ &\partial\Phi/\partial n = \cos\theta f(x) \quad \text{on} \quad \Gamma_2. \end{aligned}\right\} \tag{B 5}$$

Correspondingly, we write $Bf = \Phi(x, \zeta(x))$.

The curvature of the perturbed free surface is

$$(TY_x)_x + (TY_z)_z$$

where Y is the right-hand side of (B 4) and $T = (1 + Y_x^2 + Y_z^2)^{\frac{1}{2}}$. Hence, introducing the specified form of η into this expression and proceeding as in the derivation of (7), the linearized dynamical condition at the free surface is found to give

$$(g+\gamma\alpha^2\cos\theta)f - \gamma\cos^3\theta f'' = \omega^2 Bf. \tag{B 6}$$

An existence theory for (B 6) may be completed on the lines already demonstrated. The gist of the abstract argument is unaffected by the presence of the positive functions $\cos\theta$ and $\cos^3\theta$ weighting the terms of (B 6) and the boundary condition in (B 5). For a given α^2, the gravest frequency is seen to be given by

$$\omega_1^2 = \min_{u\in\hat{H}^1} \frac{F(u)}{G(u)},$$

where
$$F(u) = \frac{1}{b}\int_0^b \{(g+\gamma\alpha^2\cos\theta)\,u^2 + \gamma\cos^3\theta u'^2\}\,dx$$

and
$$G(u) = \max_{\xi\in H^1(\Omega)} \left\{\frac{2}{b}\int_0^b \xi(x,\zeta(x))\,u(x)\,dx - \frac{1}{b}\int_\Omega (\xi_x^2+\xi_y^2+\alpha^2\xi^2)\,dx\,dy\right\}.$$

Both $F(u)$ and $G(u)$ are positive unless u is null.

B 3. *Standing waves in brimful closed basin*

As illustrated in figure 7, the incompressible liquid fills a three-dimensional domain D, the submerged part S_1 of whose boundary is rigid. At rest, the free surface S_2 of the liquid is horizontal in the plane $y = 0$. We consider standing waves for which the equation of the perturbed free surface is

$$y = \epsilon e^{i\omega t} f(x, z),$$

we impose the edge condition

$$f = 0 \quad \text{on} \quad \Sigma = S_1 \cap S_2, \tag{B 7}$$

and mass conservation evidently requires that

$$\int_{S_2} f\,dx\,dz = 0. \tag{B 8}$$

Writing the velocity potential in the form

$$\phi = i\omega\epsilon e^{i\omega t}\psi(x, y, z),$$

we have

$$\left.\begin{aligned} &\Delta\psi = 0 \quad \text{in} \quad D, \\ &\partial\psi/\partial n = 0 \quad \text{on} \quad S_1, \\ &\psi_y(x, 0, z) = f(x, z) \quad \text{on} \quad S_2, \end{aligned}\right\} \tag{B 9}$$

where the last is required by the linearized kinematical condition at the free surface. Finally, the linearized dynamical condition at the free surface gives

$$gf - \gamma(f_{xx} + f_{zz}) = \omega^2\psi(x, 0, z), \tag{B 10}$$

the right-hand side of which corresponds, by virtue of (B 9), to a linear transformation of f, say $\omega^2 Qf$.

Solutions f are required to satisfy (B 7) and (B 8). Accordingly, they may be considered to belong to an appropriate subspace of the Sobolev space $\mathring{W}_{1,2}(S_2)$, the elements of which have L^2 generalized derivatives on S_2 and vanish (weakly) on the boundary Σ of S_2. The subspace, say $\mathscr{H}$, is defined by the condition (B 8). Hence it appears that the frequency of the gravest wave mode is given by

$$\omega_1^2 = \min_{v \in \mathscr{H}} \frac{N(v)}{M(v)}, \tag{B 11}$$

where

$$N(v) = \int_{S_2} \{gv^2 + \gamma(v_x^2 + v_z^2)\}\,dx\,dz,$$

and

$$M(v) = \int_{S_2} v\,Qv\,dx\,dz.$$

Note that $N^{\frac{1}{2}}$ is an equivalent norm for $\mathscr{H}$, so that N is a coercive, weakly lower-semicontinuous functional over $\mathscr{H}$. An explicit representation of M is

$$M(v) = \max_{\chi \in H^1(D)} \left\{2\int_{S_2} \chi(x, 0, z)\,v\,dx\,dz - \int_D |\nabla\chi|^2\,dx\,dy\,dz\right\}.$$

which shows that $M(v) > 0$ unless v is null. It can be shown also that M is weakly continuous over $\mathscr{H}$, and therefore the minimum (B 11) is achieved.

An interesting physical aspect is covered by allowing g to be negative. The theory then bears on the stability of the plane free surface of liquid in an inverted basin. Stability to infinitesimal disturbances is assured if all normal modes have real frequencies, and the limit of stability occurs when $\omega_1^2 = 0$. Thus, according to (B 11), the plane free surface subject to the edge constraint (B 7) is stable or unstable accordingly as $g > -g_0$ or $g < -g_0$, where

$$\frac{g_0}{\gamma} = \min_{v \in \mathscr{H}} \left\{ \int\!\!\int_{S_2} (v_x^2 + v_z^2)\, dx\, dz \Big/ \int\!\!\int_{S_2} v^2\, dx\, dz \right\}. \tag{B 12}$$

The method of Steiner symmetrization (Pólya & Szegö 1951) establishes that, for a given area of S_2, the minimum (B 12) is least when the boundary Σ is circular. In this case, the minimum is easily shown to be $(j_{1,1}/R)^2$, where R is the radius of Σ and $j_{1,1} = 3{\cdot}8317$ is the first positive zero of the Bessel function J_1. In terms of polar coordinates (r, θ) in the plane $y = 0$, the respective mode of displacement (i.e. the minimizing function in $\mathscr{H}$) is

$$f_1 = J_1(j_{1,1} r/R) \cos\theta. \tag{B 13}$$

Thus, considering the equilibrium of liquid in a brimful inverted vessel, where the plane horizontal free surface beneath is fixed around a circular edge, we may conclude that the equilibrium is stable to small disturbances if $R < R_c = j_{1,1}(\gamma/g)^{\frac{1}{2}} = 10{\cdot}4$ mm for water with $\gamma = 72$ mN/m. If R exceeds R_c, the equilibrium is unstable and small displacements of the free surface in the mode (B 13) will grow exponentially with time. In the case that the edge of the free surface is other than circular, the condition of stability becomes $A < A_c$, where A is surface area and the critical value A_c is larger than πR_c^2.

REFERENCES

ADAMS, R. A. 1975 *Sobolev Spaces*. Academic Press.

ASTLEY, R. J. 1969 Fluid oscillations in flexible containers. *M.Sc. Dissertation, Dept. of Mathematics, Univ. of Bristol.*

DUNFORD, N. & SCHWARTZ, J. T. 1963 *Linear Operators*, vol. 2. *Spectral Theory*. Interscience.

KRASNOLSEL'SKII, M. A. 1964 *Positive Solutions of Operator Equations*. Noordhoff.

LAMB, H. 1932 *Hydrodynamics*, 6th edn. Cambridge University Press.

LIONS, J. L. & MAGENES, E. 1968 *Problèmes aux Limites Non Homogènes et Applications*. Paris: Dunod.

PÓLYA, G. & SZEGÖ, G. 1951 *Isoperimetric Inequalities in Mathematical Physics*. Princeton University Press.

PROTTER, M. H. & WEINBERGER, H. F. 1967 *Maximum Principles in Differential Equations*. Prentice-Hall.

STAMPACCHIA, G. 1963 On some regular multiple integral problems in the calculus of variations. *Comm. Pure Appl. Math.* **36**, 383–421 (see particularly top of p. 387 and footnote).

STEPANOV, V. G., VOLYAK, L. D. & TARLAKOV, Y. U. 1977 *J. Engng Phys.* (*Inzh.-Fiz. Zh.*) **32**, 646–648.

WALBRIDGE, N. L. & WOODWARD, L. A. 1970 Phase velocity of surface capillary–gravity waves. *Phys. Fluids* **13**, 2461–2465.